arXiv:hep-lat/0206027v1 24 Jun 2002

Oxford preprint OUTP-02-27P

SU(N) gauge theories in 2+1 dimensions – further results

Biagio Lucini and Michael Teper

Theoretical Physics, University of Oxford,
1 Keble Road, Oxford, OX1 3NP, U.K.

Abstract

We calculate the string tension and part of the mass spectrum of SU(4) and SU(6) gauge theories in 2+1 dimensions using lattice techniques. We combine these new results with older results for $N_c = 2, ..., 5$ so as to obtain more accurate extrapolations to $N_c = \infty$. The qualitative conclusions of the earlier work are unchanged: SU(N_c) theories in 2+1 dimensions are linearly confining as $N_c \to \infty$; the limit is achieved by keeping $g^2 N_c$ fixed; SU(3), and even SU(2), are 'close' to SU(∞). We obtain more convincing evidence than before that the leading large-N_c correction is $O(1/N_c^2)$. We look for the multiplication of states that one expects in simple flux loop models of glueballs, but find no evidence for this.

1 Introduction

As a by-product of our recent work on k-strings in D=2+1 SU(4) and SU(6) gauge theories [1] we also calculated the lightest masses with $J^{PC} = 0^{++}, 0^{--}, 2^{++}, 2^{--}$ quantum numbers. In this note we combine these new results with the previous work of one of the authors [2] so as to obtain more accurate information about the $N_c = \infty$ limit and the N_c dependence of SU(N_c) gauge theories in D=2+1.

This note is intended as an addendum and we refer the reader to [2] as well as our related work in D=3+1 [1, 3] for a discussion of the (well-known) physics motivation [4] as well as the (mostly standard) lattice techniques.

In the next section we discuss the way our analysis differs from that of [2] and we perform a partial re-analysis of that earlier work so as to allow us to include it in a combined analysis with the new calculations. We then turn to an analysis of the string tension, σ, which is the physical quantity we calculate most accurately. We confirm that the $N_c = \infty$ limit is achieved by keeping constant the 't Hooft coupling, $g^2 N_c$, and we are able to determine quite accurately that the leading corrections are $O(1/N_c^2)$. We then analyse the glueball masses and confirm that they also show little variation with N_c. Finally we describe some calculations designed to reveal the increasing multiplication of states with increasing N_c, which is expected [5] in models where glueballs are composed of closed loops of flux. We find no evidence for this in our exploratory study.

2 Some technical details

Our lattices are cubic with periodic boundary conditions. We use the standard plaquette action

$$S = \beta \sum_p \{1 - \frac{1}{N_c} ReTrU_p\} \tag{1}$$

where the ordered product of the SU(N_c) matrices around the boundary of the plaquette p is represented by U_p. In the continuum limit this becomes the usual Yang-Mills action with

$$\beta = \frac{2N_c}{ag^2} \tag{2}$$

where we recall that g^2 has dimensions of mass in D=2+1, so that the dimensionless bare coupling, being a coupling on the scale a, is just ag^2. The simulations are performed with a combination of heat bath and over-relaxation updates, as described in [2]. Our SU(4) and SU(6) updates involve 6 and 15 SU(2) subgroups respectively. Masses are calculated from the exponential fall-off of appropriate correlators at large enough t, again as described in [2]. In Table 1 we list the values of β at which we perform calculations, together with the lattice size, L, and the value of the average plaquette. In Tables 2 and 3 we list the masses we obtain for SU(4) and SU(6) respectively.

Our present calculations differ from [2] in some technical details. Firstly, the mass calculations have been performed for fewer quantum numbers and for a more limited range of

operators. (The primary purpose of these calculations was to obtain the k-string tensions discussed in [1].) Since the mass calculations involve a variational selection of the 'best' glueball wavefunction from the basis of operators used, there is a danger that this might introduce a problem in combining the present results with those of [2]. However we shall see that the new and old SU(4) calculations agree with each other within errors which tells us that there is in fact no reason to worry.

The second difference is that we now do exponential fits to the correlation functions (as described in [3]) rather than relying on effective masses as in [2]. Again, the fact that the new and old SU(4) calculations agree with each other within errors reassures us that this introduces no significant relative bias.

Finally we use standard Gaussian error estimates rather than the somewhat idiosyncratic algorithm described and used in [2]. In order to be able to perform a unified statistical analysis of the old and new calculations, we have redone all the (relevant) continuum extrapolations in [2], obtaining the values shown in Table 4. We note that the new errors are typically about 30% smaller than those presented in [2].

3 The string tension

Our first step is to calculate the mass, $m_P(L)$, of a flux tube that winds around our $L \times L$ spatial torus, as described in [2, 1]. We then extract the string tension, σ, using

$$am_P(L) = a^2\sigma L - \frac{\pi}{6L}. \tag{3}$$

This relation assumes that we have linear confinement and that the leading correction is that of a simple periodic bosonic string [6]. In the case of SU(2) there is now rather convincing evidence [1] for both these assumptions. As an example of what one can do for larger groups, such as SU(4), we plot $am_P(L)$ as a function of L at $\beta = 28$ in Fig.1. (The masses on the smaller volumes are listed in Table 11 of [1].) We see the approximate linear rise confirming the persistence of linear confinement for $N_c = 4$. (Note that the largest string length is $16a \simeq 4/\sqrt{\sigma}$ which should be long enough to realistically address this issue.) We also see that the bosonic string correction fills in most of the deviation from linearity at larger L. We shall therefore use eqn(3) to extract the string tension from the masses of flux loops that are longer than $\simeq 3/\sqrt{\sigma}$, where one typically finds [1] that eqn(3) works well.

Having calculated the string tension as a function of β, we follow [2] and extrapolate to the continuum limit using

$$\beta_I a\sqrt{\sigma} = c_0 + \frac{c_1}{\beta_I} \tag{4}$$

where β_I is the mean field improved coupling

$$\beta_I = \beta \times \langle \frac{1}{N_c} TrU_p \rangle. \tag{5}$$

We obtain the continuum string tension from the fitted value of $c_0 = 2N_c\sqrt{\sigma}/g^2$. The values of $\sqrt{\sigma}/g^2$ thus obtained are listed in Table 5.

In Fig.2 we plot the calculated values of $\sqrt{\sigma}/g^2$ against N_c. We immediately observe that the variation approaches a linear form for larger N_c

$$\frac{\sqrt{\sigma}}{g^2} \propto N_c \tag{6}$$

and indeed is nearly linear even down to $N_c = 2$. This confirms the usual diagrammatic expectation [4] that a smooth large-N_c limit is obtained by keeping constant the 't Hooft coupling $\lambda \equiv g^2 N_c$.

We can also ask what is the power of the leading correction. To do so we fit our string tensions with the functional form

$$\frac{\sqrt{\sigma}}{g^2 N_c} = c_0 + \frac{c_1}{N_c^\alpha}. \tag{7}$$

In Fig.3 we show how the goodness of fit varies with the power α. From this we can infer that

$$\alpha = 1.97 \pm 0.21 \tag{8}$$

if we choose errors corresponding to a 20% confidence level. If we assume that the power should be an integer, then only one value is allowed: $\alpha = 2$. This is in agreement with the usual diagrammatic expectations [4].

Fitting our calculated values with $\alpha = 2$, we obtain

$$\frac{\sqrt{\sigma}}{g^2 N_c} = 0.19755(34) - \frac{0.1200(29)}{N_c^2} \tag{9}$$

This fit has a good confidence level, $\sim 70\%$. Thus, despite our smaller errors and extended range in N_c, the observation in [2] still stands: we can describe the string tension of $SU(N_c)$ gauge theories, all the way down to $SU(2)$, by that of the $SU(\infty)$ theory supplemented by the leading correction with a modest coefficient.

4 The mass spectrum

We list in Tables 2 and 3 our calculated masses. We know [7] that with the plaquette action the leading lattice correction to dimensionless ratios of physical quantities, such as $m_G/\sqrt{\sigma}$ is $O(a^2)$. Thus we extrapolate to the continuum limit using

$$\frac{m_G(a)}{\sqrt{\sigma(a)}} = \frac{m_G(a=0)}{\sqrt{\sigma(a=0)}} + ca^2\sigma. \tag{10}$$

The results are shown in Table 4. All these extrapolations have a good χ^2 apart from those indicated by an asterisk. We also show similar extrapolations for the masses calculated in [2] but with the errors recalculated as described in Section 2.

We first note that the old and new SU(4) calculations agree, within errors, for the lightest, most accurately determined states. This reassures us that the different procedures used in

these calculations do not lead to a relative systematic difference that would undermine a combined statistical analysis.

The variation of our mass ratios with N_c is weak which encourages us to try to fit with just the leading large-N_c correction:

$$\frac{m_G}{g^2 N_c} = d_0 + \frac{d_1}{N_c^2} \tag{11}$$

where $d_0 = \lim_{N_c\to\infty} m_G/g^2N_c$. The results of such fits are listed in Table 6 where we also produce corresponding values of $m_G/\sqrt{\sigma}$, which have been obtained by using eqn(9). We note that we obtain acceptable fits in all cases, except in the case of the rather heavy 2^{++} where the low value in SU(6) makes it impossible to find a good fit.

To illustrate all this we plot m_G/g^2N_c against $1/N_c^2$ for the 0^{++} and 0^{--} glueballs in Fig.4. We observe that the dependence of our masses on N_c is really very weak over the whole range of N_c.

5 Are glueballs loops of flux?

If SU(3) glueballs are composed of closed loops of fundamental (k=1) flux then in SU($N_c \geq 4$) there will be extra states composed of closed loops of $k \neq 1$ flux [5]. In simple, but natural, string models of glueballs [5, 8] the masses of such states will be scaled up by a factor of approximately $\sqrt{\sigma_k/\sigma}$, where σ_k is the k-string tension (so that $\sigma_{k=1} \equiv \sigma$). These string tensions have been recently calculated and satisfy Casimir scaling, $\sigma_k/\sigma \simeq k(N_c-k)/(N_c-1)$, to a good approximation [1]. Is there any sign of such extra states in our calculations?

We recall that our glueball operators are composed of products of highly 'smeared' SU(N_c) matrices around the boundaries of squares and rectangles [2]. When we take products of these matrices around the torus we obtain a basis of operators that typically provides a good wavefunctional for the winding fundamental flux tube and so we may regard our usual glueball operators as being closed loops of fundamental flux. To construct corresponding loops of $k = 2$ strings we take the fundamental loop, l, twice around the boundary in the form Tr($l.l$) or Trl. We can project onto the antisymmetric $k = 2$ representation, $k = 2A$, as well. We look for extra states in the $k = 2$ and $k = 2A$ bases of operators as compared to the $k = 1$ basis. We note that the lightest few states obtained in the usual $k = 1$ basis seem to continue well from $N_c = 2, 3$ to larger N_c [2] and so seem to possess no extra states at larger N_c.

We calculate the spectrum of states separately using as a basis either the usual $k = 1$ operators, or the $k = 2$ operators or the $k = 2A$ operators. We do this for SU(6) where mixings and decays, which might serve to obscure the effects we are searching for, should be weak. In SU(6) any such new states should have masses that are larger by a factor $\sim \sqrt{1.6} \simeq 1.26$. In Table 7 we show the 0^{++} states obtained using these different bases of operators. Masses are obtained from exponential fits. For heavier states, indicated by a single asterisk, we take the effective mass from $t = a$ to $t = 2a$. for the very heaviest states, indicated by a double asterisk, we take the effective mass from $t = 0$ to $t = a$. What we see is that there is no clear sign of extra states in the $k = 2A$ sector as compared to the $k = 1$ sector, in the expected mass

range. It is interesting to note that the one clear extra state in the $k = 2$ sector, with a mass of $am \simeq 1.20$, fits in well with being just the scattering state composed of two ground state 0^{++} glueballs in an S-wave. (Large-N_c counting will suppress its appearance in the $k = 1$ sector.) We have performed similar comparisons in the 0^{--} and 2^{++} sectors with similar conclusions.

Although our results look quite negative, they should be regarded as preliminary. Our operators are based on closed loops whose sizes are not much larger than the transverse extent of the smeared matrix, and which might therefore not be a good basis for closed 'string-like' states. So calculations with larger loops need to be performed. Moreover the lighter states may be smaller and may be the least string-like. Thus one needs an accurate comparison for higher mass states, which is something we would not claim to have achieved in the present calculation.

6 Conclusions

In this paper we have confirmed the main conclusions of [2] over a larger range of N_c. We have also looked for an increase in the density of states of the kind that naturally arises [5, 8] in models where glueballs are composed of closed loops of flux. In what is admittedly a crude study, we found no sign of such extra states.

One motivation for these large-N_c calculations is to provide theorists who are attempting to develop (mainly) analytic methods, with something to compare against. Thus we find it interesting to note that the string tension derived as a first approximation in [9]

$$\frac{\sqrt{\sigma}}{g^2} = \sqrt{\frac{N_c^2 - 1}{8\pi}} \tag{12}$$

is in fact extremely close to all our calculated values. As for the glueball spectrum, we note the predictions in [10] for the lightest glueball masses in the $N_c \to \infty$ limit: $m_{0^{++}} = 4.10(13)\sqrt{\sigma}$, $m_{0^{--}}/m_{0^{++}} = 1.35(5)$ and $m_{2^{++}}/m_{0^{++}} = 1.60(17)$. The first and last of these predictions are consistent with our values, while the second is only two standard deviations out. We also note that recent AdS/CFT calculations of glueball masses (see [11] for a review) are compatible with our values. Finally one should add that insights into the significance of the detailed mass spectrum may be obtained through a comparison with related D=2+1 field theories [12].

Acknowledgments

These calculations were carried out on Alpha Compaq workstations in Oxford Theoretical Physics, funded by PPARC and EPSRC grants. One of us (BL) was supported by a PPARC and then by a EU Marie Sklodowska-Curie postdoctoral fellowship.

References

[1] B. Lucini and M. Teper, Phys. Rev. D64 (2001) 105019 (hep-lat/0107007);
Phys.Lett. B501 (2001) 128 (hep-lat/0012025).

[2] M. Teper, Phys. Rev. D59 (1999) 014512 (hep-lat/9804008).

[3] B. Lucini and M. Teper, JHEP 0106 (2001) 050 (hep-lat/0103027).

[4] G. 't Hooft, Nucl. Phys. B72 (1974) 461.
E. Witten, Nucl. Phys. B160 (1979) 57.
S. Coleman, 1979 Erice Lectures.
A. Manohar, 1997 Les Houches Lectures, hep-ph/9802419.
S.R. Das, Rev. Mod. Phys. 59(1987)235.
M. Teper, hep-ph/0203203.

[5] R. Johnson and M. Teper, hep-ph/0012287.

[6] M. Luscher, K. Symanzik and P. Weisz, Nucl. Phys. B173 (1980) 365.
Ph. de Forcrand, G. Schierholz, H. Schneider and M. Teper, Phys. Lett. B160 (1985) 137.

[7] K. Symanzik, Nucl. Phys. B226 (1983) 187; *ibid.* 205.

[8] N. Isgur and J. Paton, Phys. Rev. D31 (1985) 2910.

[9] V.P. Nair, hep-th/0204063.
D. Karabali and V.P. Nair, Nucl. Phys. B464 (1996) 135; Int. J. Mod. Phys. A12 (1997) 1161.
D. Karabali, C. Kim and V.P. Nair, hep-th/9705087.

[10] S. Dalley and B. van de Sande, Phys. Rev. D63 (2001) 076004 (hep-lat/0010082).

[11] J. Terning, hep-ph/0204012.

[12] M. Caselle, M. Hasenbusch, P. Provero and K. Zarembo, Phys.Rev. D62 (2000) 017901 (hep-th/0001181).
M. Caselle, M. Hasenbusch and P. Provero, Nucl. Phys. Proc. Suppl. 63 (1998) 616 (hep-lat/9709087).

SU(4)			SU(6)		
β	L	plaq	β	L	plaq
60.0	32	0.914426(2)	108.0	24	0.887953(2)
45.0	24	0.884724(3)	75.0	16	0.835392(6)
33.0	16	0.840190(7)	60.0	12	0.790321(8)
28.0	16	0.809332(6)	49.0	10	0.736809(12)
28.0	12	0.809350(15)	42.0	8	0.684495(20)
21.0	10	0.737640(15)			
18.0	8	0.68593(4)			

Table 1: Average SU(4) and SU(6) plaquette values for the new calculations.

state	$\beta = 18$ L=8	$\beta = 21$ L=10	$\beta = 28$ L=12	$\beta = 28$ L=16	$\beta = 33$ L=16	$\beta = 45$ L=24	$\beta = 60$ L=32
l	1.50(2)	1.223(11)	0.715(4)	0.9937(58)	0.6622(29)	0.4974(22)	0.3571(14)
0^{++}	1.85(6)	1.54(4)	1.057(15)	1.082(11)	0.872(10)	0.620(5)	0.4592(27)
0^{++*}	2.5(3)	2.29(15)	1.53(3)	1.56(4)	1.289(23)	0.940(8)	0.682(4)
0^{++**}	–	2.58(34)	1.77(5)	1.88(6)	1.506(24)	1.117(33)	0.842(5)
0^{--}	2.7(5)	2.11(14)	1.61(3)	1.53(5)	1.306(22)	0.895(20)	0.6736(34)
0^{--*}	–	2.16(26)	1.97(9)	1.96(14)	1.65(4)	1.233(16)	0.852(14)
2^{++}	–	2.4(3)	1.5(2)	1.81(5)	1.502(26)	1.051(12)	0.773(6)
2^{++*}	–	–	2.35(16)	2.23(11)	1.71(6)	1.22(6)	0.887(18)
2^{--}	–	–	2.03(11)	2.21(22)	1.81(5)	1.228(13)	0.921(10)

Table 2: Masses of glueballs, labelled by J^{PC}, and of the periodic flux loop, l, of length L : in SU(4) at the indicated values of β on lattice volumes L^3.

state	$\beta = 42$ L=8	$\beta = 49$ L=10	$\beta = 60$ L=12	$\beta = 75$ L=16	$\beta = 108$ L=24
l	1.453(14)	1.194(9)	0.8575(47)	0.6825(31)	0.4552(13)
0^{++}	1.754(54)	1.491(31)	1.161(16)	0.8885(42)	0.5925(26)
0^{++*}	2.7(7)	2.13(13)	1.752(60)	1.347(18)	0.8769(57)
0^{++**}	–	2.58(34)	1.97(9)	1.605(27)	1.1226(83)
0^{--}	2.50(27)	2.20(13)	1.707(43)	1.284(17)	0.861(8)
0^{--*}	–	2.8(4)	2.14(11)	1.66(4)	1.119(12)
2^{++}	2.6(4)	2.6(4)	1.92(7)	1.478(23)	0.953(16)
2^{++*}	–	–	2.40(16)	1.82(6)	1.242(11)
2^{--}	–	–	2.3(2)	1.79(5)	1.197(10)

Table 3: Masses of glueballs, labelled by J^{PC}, and of the periodic flux loop, l, of length L : in SU(6) at the indicated values of β on lattice volumes L^3.

$m_G/\sqrt{\sigma}$						
state	SU(2)	SU(3)	SU(4)	SU(5)	SU(4)	SU(6)
0^{++}	4.716(21)	4.330(24)	4.239(34)	4.180(39)	4.235(25)	4.196(27)
0^{++*}	6.78(7)	6.485(55)	6.383(77)	6.22(8)	6.376(45)	6.20(7)
0^{++**}	8.07(10)	8.21(10)	8.12(13)	7.87(18)	7.93(7)	8.22(12)
0^{--}		6.464(48)	6.27(6)	6.06(11)	6.230(44)	6.097(80)
0^{--*}		8.14(8)	7.84(13)	7.85(15)	8.20(15)*	7.98(15)
2^{++}	7.81(6)	7.12(7)	7.14(8)	7.15(12)	7.17(8)	6.67(18)
2^{++*}			8.50(17)	8.56(15)	8.06(22)	8.89(20)
2^{--}		8.73(10)	8.25(21)	8.25(18)	8.49(13)	8.52(20)

Table 4: Glueball masses in units of the string tension, in the continuum limit. Reanalysis of [2] on left; new calculations on right.

group	c_0	c_1	$\sqrt{\sigma}/g^2$
SU(4)	6.072(16)	-8.19(45)	0.7590(20)
SU(6)	14.000(38)	-46.5(2.6)	1.1667(32)
SU(2)	1.3405(31)	-0.417(24)	0.3351(8)
SU(3)	3.3182(61)	-2.43(11)	0.5530(10)
SU(4)	6.065(21)	-7.74(73)	0.7581(26)
SU(5)	9.657(38)	-21.4(1.9)	0.9657(38)

Table 5: Continuum extrapolations of $\beta_I a\sqrt{\sigma} \to 2N_c\sqrt{\sigma}/g^2$ as in eqn(3). New calculations (top) and reanalysed old calculations (bottom).

state	$\lim_{N_c\to\infty} m/g^2N_c$	slope	$N_c \geq$	χ^2/n_{df}	$\lim_{N_c\to\infty} m/\sqrt{\sigma}$
0^{++}	0.8116(36)	-0.090(28)	2	0.9	4.108(20)
0^{++*}	1.227(9)	-0.343(82)	2	0.8	6.211(46)
0^{++**}	1.65(4)	-2.2(7)	4	1.6	8.35(20)
0^{--}	1.176(14)	0.14(20)	3	0.2	5.953(71)
0^{--*}	1.535(28)	-0.35(35)	3	1.0	7.77(14)
2^{++}	1.359(12)	-0.22(8)	2	2.9	6.88(6)
2^{++*}	1.822(62)	-3.9(1.3)	4	0.4	9.22(32)
2^{--}	1.615(33)	-0.10(42)	3	1.0	8.18(17)

Table 6: The large N_c limit of the mass spectrum in units of g^2N_c; with the slope of the linear fit when plotted against $1/N_c^2$. Also the range of colours fitted and the χ^2 per degree of freedom of the best fit. Last column uses the value of $\lim_{N_c\to\infty}\sqrt{\sigma}/g^2N_c$ in eqn(9).

am_{eff} ; $J^{PC} = 0^{++}$		
$k = 1$; 10 ops	$k = 2A$; 10 ops	$k = 2$; 20 ops
0.592(4)	0.594(4)	0.593(4)
0.88(1)	0.90(1)	0.89(1)
1.14(1)	1.17(1)	1.13(1)
		1.20(1)
1.30(2)	1.29(6)	1.31(2)
1.47(2)*	1.42(2)*	1.46(2)*
1.53(2)*		1.49(2)*
1.78(4)*	1.76(4)*	1.72(4)*
		1.73(4)*
		1.65(3)*
		1.72(4)*
2.9(2)**	2.9(2)**	2.3(1)*

Table 7: Spectrum of scalar masses at $\beta = 108$ in SU(6) obtained using operators based on fundamental flux loops ($k = 1$) doubly charged loops ($k = 2$) and from the antisymmetric combination of the latter ($k = 2A$). States are listed in the order of effective masses from $t = 0$ to $t = a$ and are matched to guide the eye.

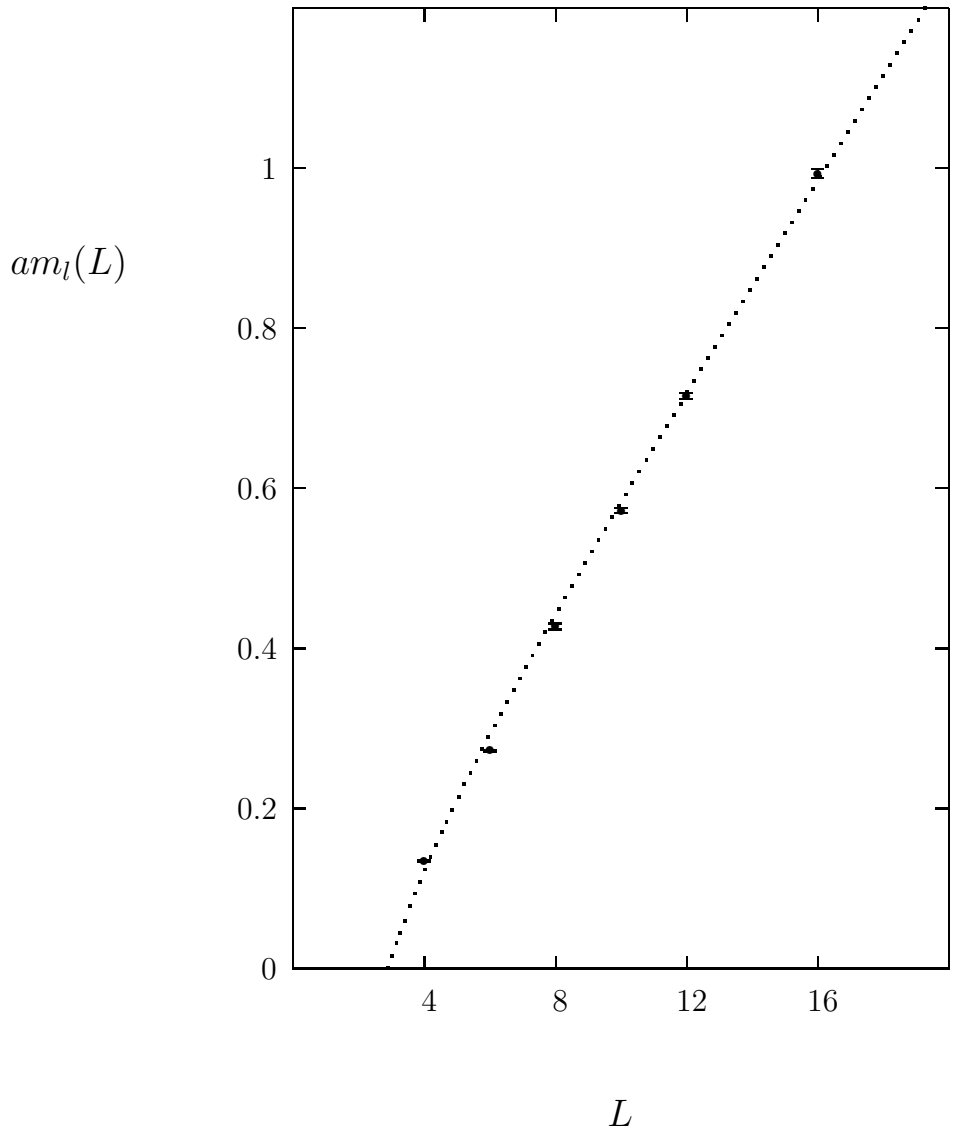

Figure 1: The mass of a periodic flux loop of length aL at $\beta = 28$ in SU(4). The line shows a fit of the form in eqn(3).

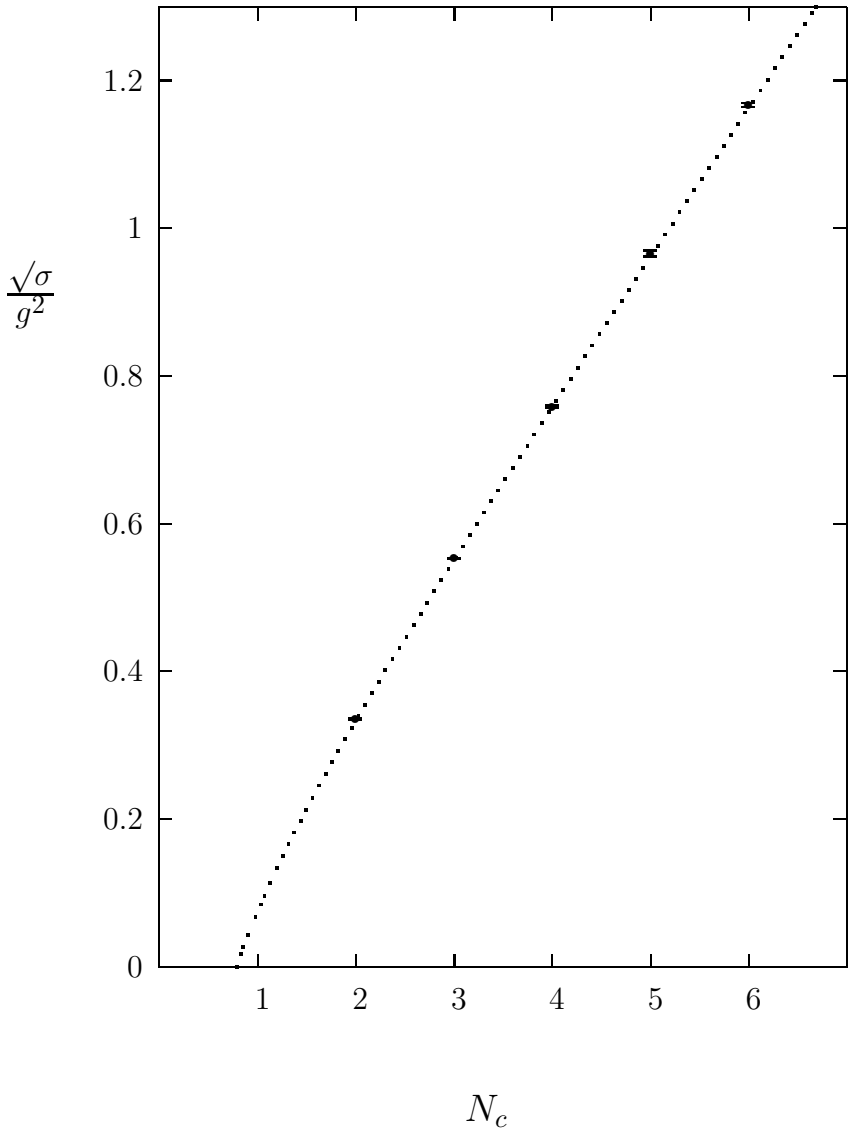

Figure 2: The value of $\sqrt{\sigma}/g^2$ as a function of N_c. The line shows the fit in eqn(9).

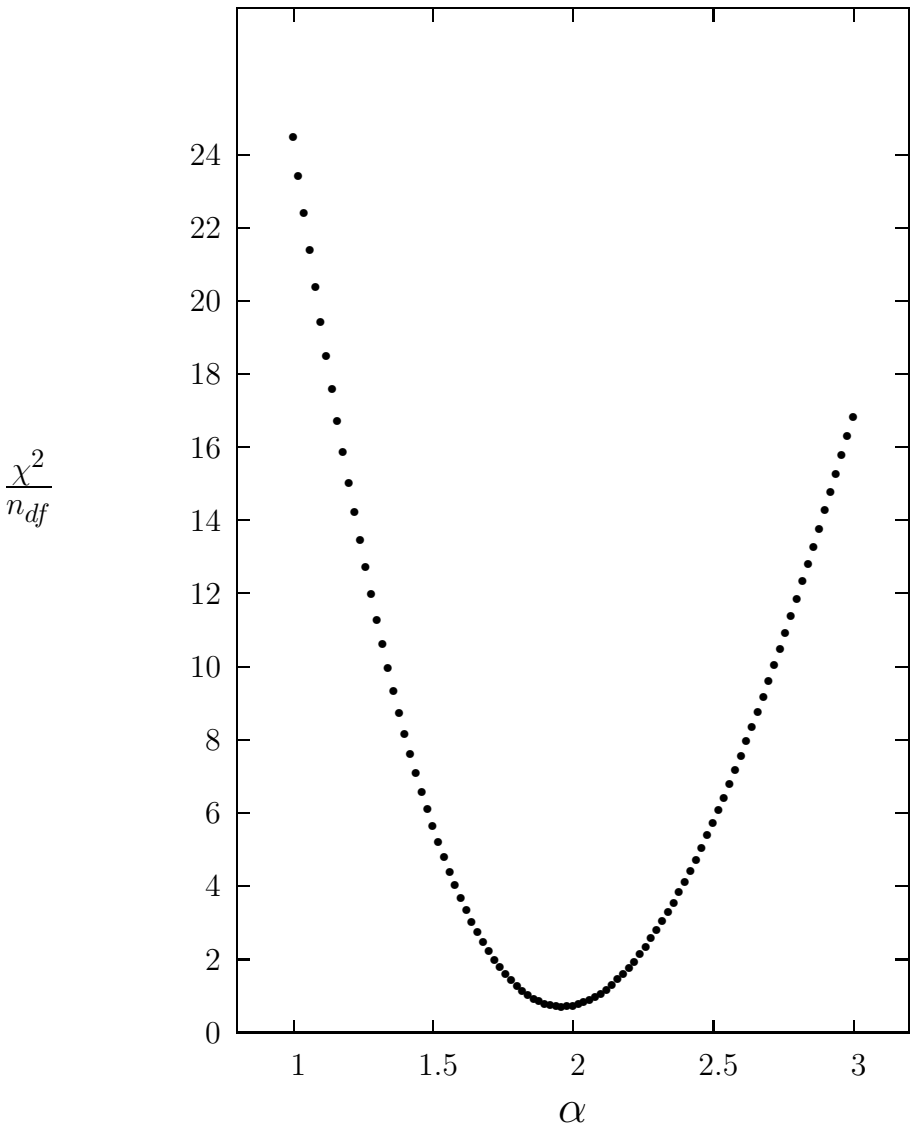

Figure 3: The χ^2 per degree of freedom against the power, α, of the leading large-N_c correction when fitting $\sqrt{\sigma}/g^2N_c$ to eqn(7).

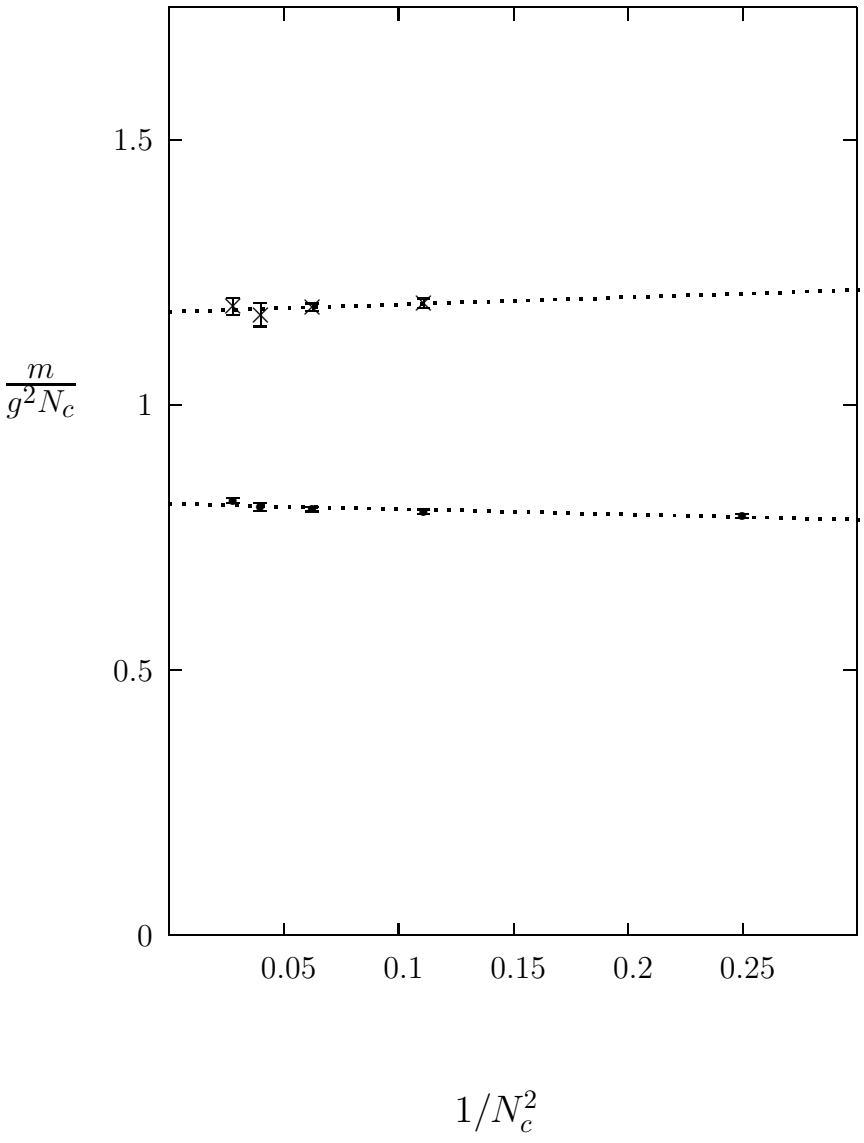

Figure 4: $0^{++}(\bullet)$ and $0^{--}(\times)$ glueball masses in units of $g^2 N_c$, plotted against $1/N_c^2$. The best linear extrapolations to the $N_c = \infty$ limit are shown.